Ultrathin, Oil-Compatible, Lubricious Polymer Coatings

A Comparison of Grafting-To and Grafting-From Strategies

Journal Article

Author(s):
Bielecki, Robert M.; Doll, Patricia; Spencer, Nicholas D.

ORIGINAL PAPER

Ultrathin, Oil-Compatible, Lubricious Polymer Coatings: A Comparison of Grafting-To and Grafting-From Strategies

Robert M. Bielecki · Patricia Doll · Nicholas D. Spencer

Abstract A grafting-to approach is described as a means of fabricating ultrathin, oil-compatible, friction-reducing coatings. The tribological properties of grafted-to coatings of poly(dodecyl methacrylate) (P12MA), prepared by means of a photoactivated perfluorophenylazide adhesion promoter, were compared with those of grafted-from coatings of the same polymer of comparable molecular weight, prepared via surface-initiated, atom-transfer radical polymerisation. It was shown that in a sub-hydrodynamic regime (i.e. boundary/brush lubrication), both coating types can be equivalently effective, exhibiting very low friction coefficients (0.02) against a bare silica countersurface with no detectable wear over the duration of the test (around 1,000 cycles, and maximal Hertzian contact pressure ca 170 MPa as calculated for a bare–bare configuration), providing that sufficiently viscous base lubricants are employed.

Keywords Polymer brush · Oil lubrication · Grafting-to · Grafting-from · Poly(dodecyl methacrylate) · Perfluorophenylazide

1 Introduction

Polymer chains, when attached to a surface at sufficiently high grafting densities and under good solvent conditions, undergo stretching in the direction perpendicular to the surface to form polymer brushes. Such systems have been identified as friction-reducing coatings [1, 2]. Tethering of

polymeric chains to the surface can be achieved by two main approaches: either by attaching *pre*-synthesised polymer chains (grafting-to) or by conducting polymer synthesis initiated from the surface, leading to the outgrowth of polymer chains (grafting-from).

Grafting-to is generally an experimentally less-demanding approach, as the polymers to be attached can, in principle, be purchased. In contrast, surface-initiated polymerisation (SIP) involves the complexities of polymer synthesis on the surface of interest [3]. Due to steric effects, however, the grafting-to approach has an upper limit on grafting density, as macromolecules already grafted to the surface hinder the attachment of further chains. With the grafting-from strategy, single monomers can readily be incorporated into much more densely packed growing chains.

For grafting-from, firm attachment with the surface is achieved via bifunctional molecules containing a reactive group capable of initiating polymerisation and an anchoring group that interacts with the substrate material, e.g., thiols on gold, silver, copper or platinum [4, 5], catechols on steel surfaces [6] or silanes on silicon wafers [7].

In the case of grafting-to, the attachment of macromolecules is generally achieved by surface-anchoring groups present on the polymer and may be different in nature, i.e. electrostatic as in the case of poly(L-lysine)-*g*-poly(ethylene glycol) (PLL-*g*-PEG) on negatively charged oxides [8] or coordinative for catechol-based molecules [9]. In contrast, this study focuses on spin-coated polymeric films that are grafted onto surfaces via photocoupling. A comparison of their tribological properties is made with previously reported, grafted-from, oil-compatible friction-reducing polymer brushes [10, 11] of very similar composition.

The reported PFPA-based photocoupling chemistry [12, 13] is a robust grafting-to technique, in which the polymer coating is immobilised onto the surface by means of

R. M. Bielecki · P. Doll · N. D. Spencer (✉)
Laboratory for Surface Science and Technology, Department of Materials, ETH Zurich, Wolfgang-Pauli-Strasse 10, 8093 Zurich, Switzerland
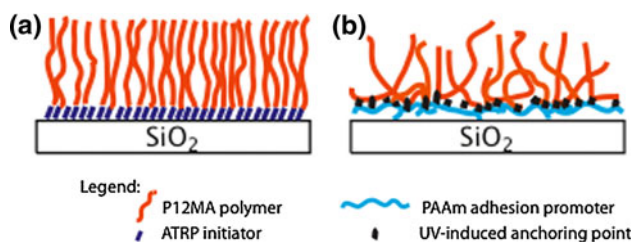e-mail: spencer@mat.ethz.ch; nspencer@ethz.ch

Fig. 1 Schematic presentation of the polymer coatings' structures. **a** Uniform linear chains obtained via SI-ATRP, **b** disordered structure with multiple chain insertions obtained via PFPA-based grafted-to method. Detailed description of fabrication is contained in Fig. 2

nitrene groups that are photochemically produced from an immobilised azide. The nitrene groups carry out non-selective radical insertion into the C–H bonds of polymer chains that have been previously spin-coated onto the surface. Coatings of this type are characterised by a generally low degree of order, the possibility of multiple surface attachments occurring within a single chain, and a broader distribution of free chain lengths extending from the surface. Compared to grafted-from brushes, this apparently more haphazard (though very reproducible) approach of PFPA-based surface functionalisation (schematically depicted in Fig. 1) has the considerable advantage of simplicity, which prompted us to examine its tribological properties in detail. To benchmark the applicability of grafted-to P12MA coatings, their lubricating properties were compared with those obtained for polymer brushes of similar thickness grafted from the surface using surface-initiated atom transfer radical polymerisation (SI-ATRP)—a variety of controlled radical polymerisation (CRP) [14].

2 Experimental

2.1 Materials

Poly(dodecyl methacrylate) (P12MA) solution [25 wt% in toluene, analytical standard, average M_w 470,000 (Typical), average M_n 150,000 (Typical)] and poly(allyl amine) (PAAm) hydrochloride (molecular weight 14 kDa) were purchased from Sigma Aldrich, Switzerland. Perfluorophenylazide-N-hydroxysuccinimide (PFPA-NHS) was kindly donated by SuSoS AG, Switzerland. 4-(2-Hydroxyethyl) piperazine-1-ethanesulfonic acid (Fluka, Switzerland) was used to prepare a 10 mM buffer solution, the pH being set to 7.4 (HEPES 1).

The remaining materials were used as described in a previous study [10].

2.2 Surface Functionalisation

2.2.1 Grafting-To Approach

2.2.1.1 Adhesion-Promoter Preparation
The azide-containing adhesion promoter, PAAm–PFPA, was prepared by dissolving 12.66 mg PAAm hydrochloride in 2.53 ml MilliQ water, to which 31.64 mg potassium carbonate was added, followed by heating to boiling to ensure a complete dissolution of the polymer. Separately, 11.24 mg PFPA-NHS was mixed with 2.6 ml ethanol and sonicated for 5 min. Afterwards, the PFPA solution was added to the PAAm solution. The mixture was stirred overnight and shielded from light with aluminium foil (photocoupling agents are highly sensitive to light and should be used within 1 week).

2.2.1.2 Functionalisation with Adhesion Promoter
Silicon wafers were washed with toluene and isopropanol (each 2 times for 10 min in an ultrasonic bath) and blown dry with nitrogen, followed by 30 min in an ozone cleaner (UV/Ozone ProCleaner™ and ProCleaner™ Plus, BioForce, IA, USA). Such pre-cleaned wafers were incubated for 30 min in a 0.1 mg/ml solution of the PAAm–PFPA adhesion promoter in HEPES 1/ethanol (2:3 ratio). Afterwards, samples were rinsed first with a fresh HEPES 1/ethanol solution, followed by ultrapure MilliQ water. After adsorption of the adhesion promoter, samples were stored in the dark.

2.2.1.3 Spin Coating and Curing of P12MA
A solution of P12MA in toluene was spin-coated (4,000 rpm, ca 150 μl of polymer solution, 30 s, using a Fairchild Technologies GmbH, Germany spin-coater equipped with a COROS OP15 controller, Siemens, Germany) onto the adhesion-promoter-functionalised surfaces. The spin-coated films were irradiated with UV light ($\lambda = 254$ nm) for 2 min at ca. 0.8 mW/cm². After UV-curing, samples were washed multiple times with toluene (including an overnight incubation), to remove uncoupled polymer chains.

2.2.2 Grafting-From Approach

The two-step surface functionalisation, consisting of 11-(2-bromo-2-methyl-propionyl)-dimethylchlorosilane (BPCS) silanisation and SI-ATRP synthesis of the P12MA coating (Fig. 2a) followed the protocol previously reported for silicon wafers and glass borosilicate balls [10]. The desired coating thickness was dictated by a synthesis time set to 8 min [11].

2.3 Lubricating Fluids

Hexadecane (kinematic viscosity ca. 4 cSt), as well as two additive-free ester oils (EO) and two additive-free
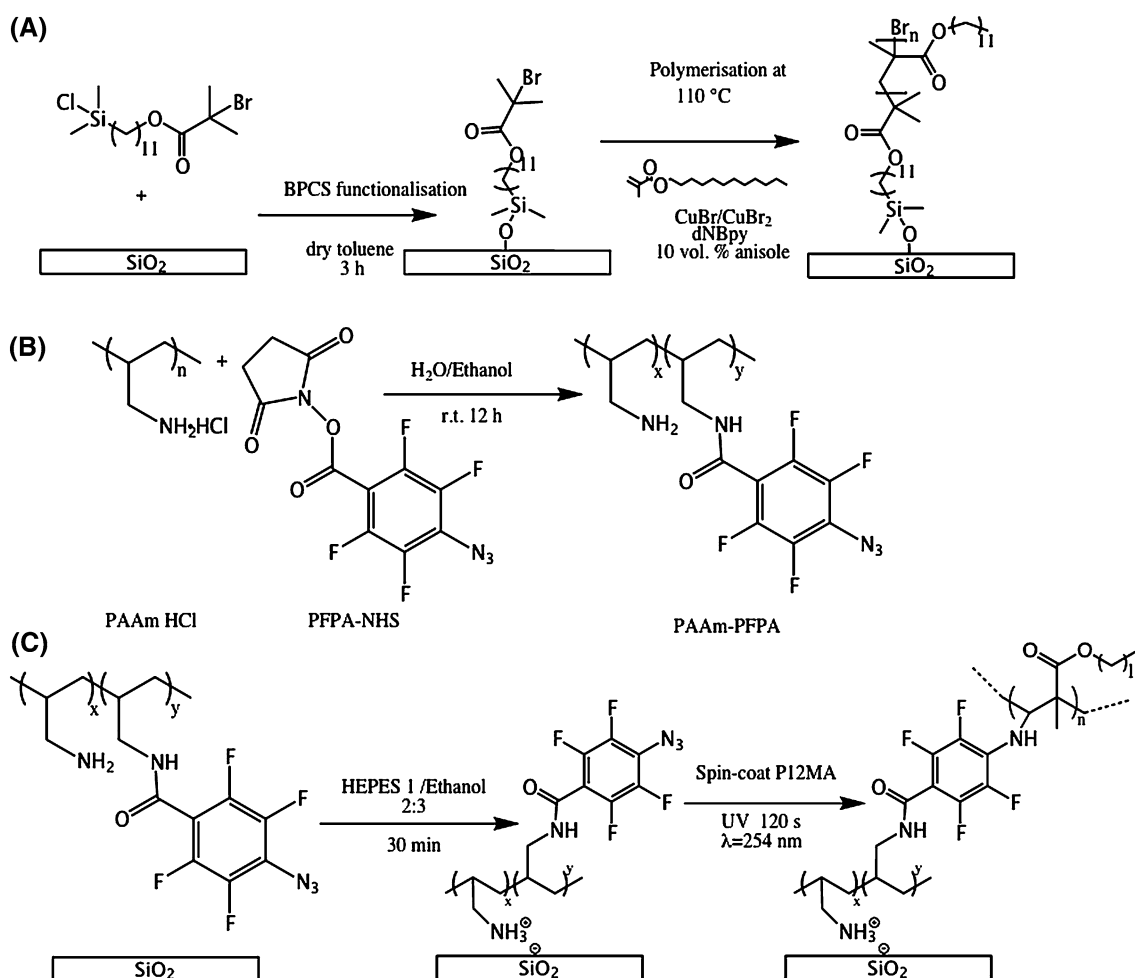
Fig. 2 Surface functionalisation schemes. **a** Grafting-from: deposition of an ATRP BPCS initiator molecule and SI-ATRP reaction. **b** Synthesis of a PAAm–PFPA adhesion promoter. **c** Grafting-to: deposition of an adhesion promoter, followed by spin-coating and UV curing of P12MA coating (one possible result of a radical insertion is depicted)

petroleum fraction (PF) oils, characterised by kinematic viscosities (at 20 °C) of 500 cSt (named EO500), 1,000 cSt (named EO1000), 36 cSt (named PF36) and 350 cSt (named PF350), were used.

Before starting tribological experiments, a few drops of lubricant were deposited on a disc, so as to cover the entire intended sliding track, after which a ball was brought close to the surface, allowing a meniscus to be established. Such evenly wetted samples were allowed to equilibrate with the solvent for 10 min prior to the application of contact pressure.

2.4 Lateral Force Microscopy

Lateral forces were measured with an MFP-3D atomic force microscope (Asylum Research, Santa Barbara, CA). Measurements were carried out in *n*-hexadecane. Colloidal probes [15] were prepared by mounting SiO_2 (silica) colloidal spheres (Kromasil, Brewster, NY, diameter = 15 ± 0.5 μm) onto tipless silicon cantilevers (MICROMASH, San Jose, CA) by means of a UV-curable adhesive. The normal stiffness (0.205 N/m) of the cantilever was found by means of the thermal-tuning technique, incorporated into the AFM software.

Normal and lateral sensitivities were used to convert the position-sensitive-photodiode-generated signal (in Volts) into Newtons for normal- and lateral-force measurements, respectively. The normal sensitivity of the colloidal probe was measured by determining the slope of the curve when a colloidal probe is pressed against a hard (SiO_2) surface. Lateral sensitivity and torsional spring constant were obtained according to Cannara et al. [16], the former being determined by pressing the colloidal probe laterally against a large hard sphere and measuring the deflection of the cantilever. The frictional response reported here for each

load is the average of 5–10 line scans of 5 μm at a minimum of three different locations. The friction force for each scan is calculated by averaging the forward and reverse friction forces as (friction force forward − friction force reverse)/2.

The bare sample used for reference was cleaned as follows: 2×10 min ultrasonication in 2-isopropanol, 5 min in a piranha solution (7:3 H_2SO_4:H_2O_2) directly before friction measurements.

2.5 Tribological Studies—Tribometer

Tribological studies were performed with a NTR2 tribometer (CSM Instruments, Peseux, Switzerland) in a ball-on-disc configuration. More detailed information on the tribometer as well as data processing can be found in our previous publication [10]. In this study, all tests were performed in a bare–bare or polymer–bare configurations, where the borosilicate glass ball (2 mm in diameter, Hauser Optik, Germany) used as a countersurface was always used as an unmodified (bare) surface.

All tests were carried out in linear reciprocating mode (constant speed between direction changes, i.e. triangle wave in displacement) with an amplitude of 1 mm (i.e. 1 cycle covering a total of 4 mm). In all tests, a load of 20 mN was applied (yielding maximal Hertzian contact pressure of ca 170 MPa, as calculated for bare–bare contact); for endurance testing, a constant speed of 0.1 cm/s was used. Stribeck-like curves were collected at constant load, starting at high sliding speed (4 cm/s), then moving to successively lower sliding speeds, through the lowest sliding speed (0.01 cm/s), after which the sliding speeds were increased again, back to the highest values. 30 cycles were performed at each speed and the COF (calculated as lateral force/normal force) was averaged over the last 20 cycles (due to a startup period for the tribometer, before the set amplitude is reached). After each set of measurements at a given speed, the tribometer was stopped, and the load removed and reapplied before commencing sliding at another sliding-speed value.

2.6 Ellipsometry

A variable-angle spectroscopic ellipsometer (VASE) (M-2000F, LOT Oriel GmbH, Darmstadt, Germany) was used to determine the degree of initiator deposition and the dry thickness of the surface-bound polymers. The wavelength range for which fitting was performed lay between 370 and 995 nm and the refractive index of the coating was assumed to be 1.45 using a Cauchy model $n(\lambda) = 1.45 + 0.01/\lambda^2$ [17].

Table 1 Results of the dry thickness ellipsometric measurements and static water contact angles measurements after each functionalisation steps

Coating type	Dry thickness (nm)	Water contact angle
Si–PAAm–PFPA	2.0 ± 0.5	$46° \pm 1°$
Si–PAAm–PFPA–P12MA (GT15)	15.8 ± 0.4	$102° \pm 1°$
Si–BPCS	1.8 ± 0.1	$77° \pm 2°$
Si–BPCS–P12MA (GF30)	30.8 ± 1.1	$102° \pm 2°$

3 Results and Discussion

3.1 Coating Formation

The efficacy of the two-step surface functionalisation process—first with adhesion promoter or ATRP initiator and second with P12MA polymer—was determined by thickness and static water-contact-angle measurements. For both grafting-to and grafting-from, the final coating was highly hydrophobic, with water contact angles above 100° (Table 1).

For the two coating types, the number of chains per nm^2 and molecular weights can be estimated. First, for the grafted-to polymer chains, knowing the dry thickness (13.8 nm) of the coating and the molecular weight of the polymer (150 kDa), and assuming the density of P12MA to be 0.929 g/cm³, the grafting density of the grafted-to system can be calculated as 0.05 chains/nm^2. Second, for the grafted-from system (29 nm dry thickness), the molecular weight is estimated at 60 kDa, when assuming grafting densities of ca 0.27 chains/nm^2 [10]. It is also important to realize that the GT method is capable of tethering chains at any position along the polymer chain, as well as carrying out multiple radical insertions (attachment points) along a single chain of P12MA, intrinsically leading to a more complex structure (with possible polymer loops) for which the mean length of an average mobile polymer segment is much more broadly distributed when compared to a GF-fabricated brush.

3.2 Tribological Performance

Lateral-force-microscopy results are presented in Fig. 3. The two polymer-modified silicon surfaces yielded significantly lower frictional forces than the bare silicon wafer (covered with native oxide) when tested in hexadecane against a bare silica sphere.

Coefficient-of-friction values were obtained as the slope of a line, fitted to the points with the least-mean-square-error method. The grafted-from sample was characterised by COF = 0.05 ± 0.01 and the grafted-to P12MA coating
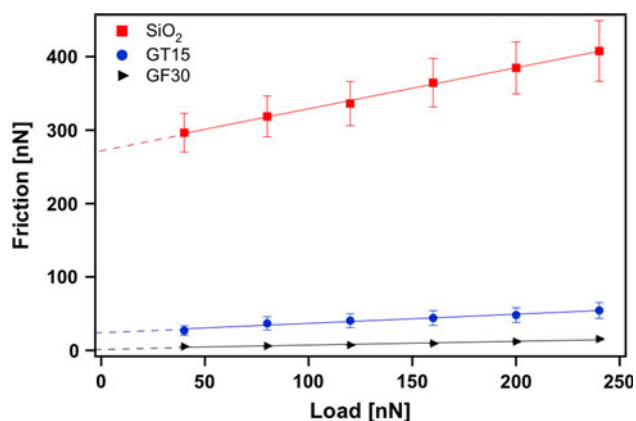
Fig. 3 Lateral-force microscopy in hexadecane for a bare silica sphere slid against a bare silicon wafer ("SiO₂"), and grafted-to ("GT15") and grafted-from ("GF_30") polymer coatings, in which the numbers approximate the dry thickness of the coating in nm. *Scan rate* 1 Hz across 5-μm scan line. 5–10 friction loops measured at each load

Fig. 4 Coefficient of friction evolution with sliding distance (*Endurance test*) for grafted-to P12MA-coated silicon wafers slid against a bare borosilicate glass ball. Load 20 mN, sliding speed 0.1 cm/s, maximal Hertzian contact pressure for bare–bare case ca 170 MPa

displayed a value of 0.13 ± 0.01 in hexadecane. The difference between the polymer coatings may arise from the higher brush thickness of GF30, or could be related to the more compact molecular arrangement of the ATRP coatings on the surface. Presumably, the inherent disorder of grafted-to surfaces could also hinder facile motion of the colloidal probe across the surface by increasing contact area and therefore adhesion. Support for the brush-thickness argument can be found in the literature [18], while the contact-area hypothesis is supported by extrapolating the linear fit towards the 0-load axis; at zero load, the grafted-to system exhibits a non-zero friction force, indicating an apparently increased adhesion contribution. This is presumably due to the greater possibility of contact between the colloid and the polymer chains in the case of the more uneven, conformal surface, than for a perfectly smooth surface of the same material. For the grafted-from system the extrapolated linear fit cuts through the (0,0) point at the graph, corresponding to a negligible adhesive component to the friction.

Nano-scale frictional experiments were followed by experiments on a micro-scale, where the Hertzian contact radii predicted for bare–bare systems are on the order of micrometres. First, the grafted-to coatings (GT15) were measured in three different lubricants (hexadecane, and two ester oils of 500 and 1,000 cSt viscosity), and slid against a bare borosilicate ball in an endurance test, in which the speed was maintained at a constant value of 0.1 cm/s (using a triangular sliding function).

The 15-nm dry-thickness, grafted-to P12MA polymer coating showed very promising lubricious properties when studied in EO500 and EO1000 lubricating fluids. The measured coefficient of f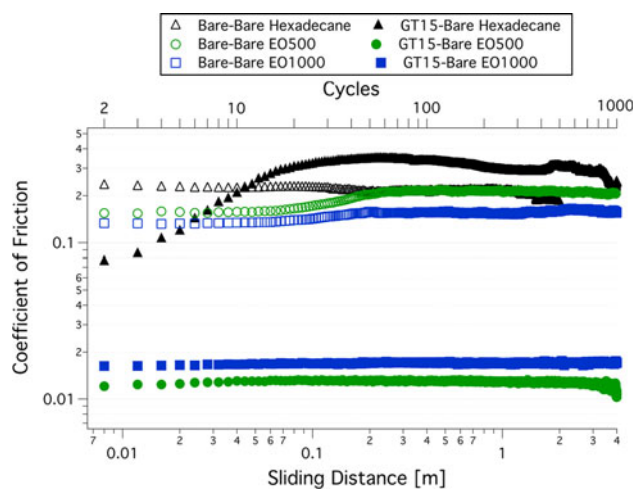riction values against bare silica spheres were an order of magnitude lower than those observed for a bare–bare configuration under the same testing conditions, at levels below 0.02 (Fig. 4). When the sliding was performed in hexadecane, the coefficient of friction values increased above 0.2 (level of the bare–bare system) within the first few centimetres of sliding, which was attributed to wearing-off of the coating.

For comparison, in endurance tests conducted under hexadecane, EO500 and EO1000 as lubricants, the 15-nm-thick grafted-to coatings (GT15) showed behaviour similar to that of coatings prepared with the SI-ATRP protocol (GF30, or 15-nm-thick GF15 for more direct comparison). Further, the coefficient of friction values observed for the ultrathin grafted-to and grafted-from coatings (dry thickness ≤30 nm) slid against a bare borosilicate ball in EO500 and EO1000 were as low as those observed for grafted-from coatings in *brush–brush* configurations of much higher thickness (≈ 250 nm) in either hexadecane or more viscous oils [10].

The significant differences in the endurance test in hexadecane and in EO500 oil prompted further tests with oils of intermediate viscosity, to identify the minimal oil viscosity that is able to deliver a satisfactory low-wear behaviour.

Application of lubricants of intermediate viscosities (PF36 and PF350) resulted in a less rapid COF increase than that observed when using hexadecane, usually reaching COF values typical for a bare–bare system in the boundary regime within the first 2–3 m of sliding. Similar stability behaviour was observed for both GT15 and GF30 coatings (GF30 slightly higher endurance, related to the coating thickness). Representative curves are presented in Fig. 5.
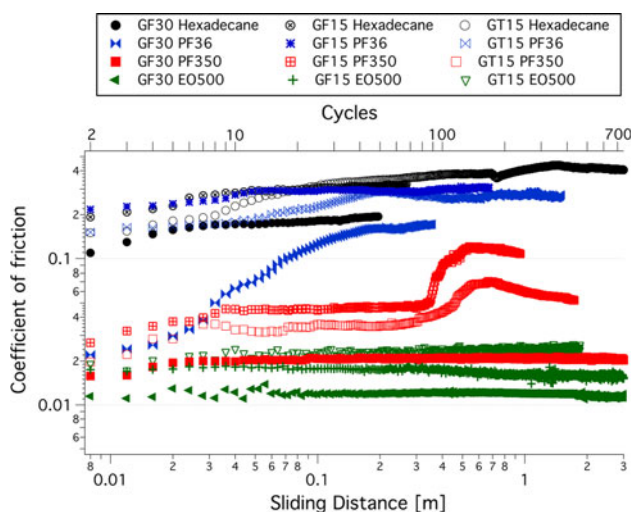
Fig. 5 Endurance tests in intermediate-viscosity oils; for grafted-to 15-nm-thick P12MA (GT15) and the grafted-from 15- and 30-nm-thick coatings (GF15 and GF30). In both the cases, sliding was carried out against an unmodified borosilicate glass ball at a constant speed 0.1 cm/s and 20-mN load

Fig. 6 Stribeck-like curves obtained in EO500 oil under 20-mN load. First, polymer-coated substrates are tested at high, moderate and then low speeds (in this order, *triangles* pointing to the *left*), after testing at 0.01 cm/s, the order is reversed and the test finishes at high speeds (*triangles* pointing to the *right*). Between each speed change, the contacts were separated and load reapplied. The COF measured for a bare–bare contact pair is presented for reference. While returning to high speed, the worn-off GT15 coating follows values typical for the bare–bare system

Fig. 7 Stribeck-like curves obtained in EO1000 oil under 20-mN load. Both functionalisation methods (GF30 and GT15) allowed a low-coefficient-of-friction regime to be maintained at low speeds. Both surfaces were able to endure the complete testing routine, evidenced by the complete reversibility of the curves

Testing conditions of 0.1 cm/s and 20 mN do not allow the endurance performance of the thin films in the highly viscous oils (EO500 and EO1000) to be differentiated. In order to investigate any potential differences, Stribeck-like curves were obtained. *A cautious analysis of such graphs is required, since the results represent both phenomena that are purely a function of viscosity, load, and speed, as well as dynamic effects such as coating degradation.* In an attempt to separate these two components clearly, a procedure in which speed is changed from high to low and again from low to high values, with 30 cycles at each speed, was performed. Figure 6 shows the results obtained for the EO500 oil. It is apparent that, under the conditions used for endurance tests (sliding speed of 0.1 cm/s), both GT15 and GF30 lead to a beneficial effect on friction, attributable to the low-friction brush regime of the polymer coatings. At speeds below 0.1 cm/s, the COF obtained for GF30 remains in the low region, while for the GT15 a gradual increase in the COF values (being an average from 20 last cycles from the 30 performed at each speed) is observed. Severe coating damage is observed at 0.01 cm/s, indicated by the high COF value of ca 0.12. Coating removal (for GT15) is confirmed by the high coefficient-of-friction values observed while increasing the speed up to the higher values—no friction-reducing effect attributable to the presence of a brush coating was observed.

A similar experiment performed in EO1000 oil (Fig. 7) showed complete reversibility of the speed-COF curve for both GF30 and GT15 functionalised samples.

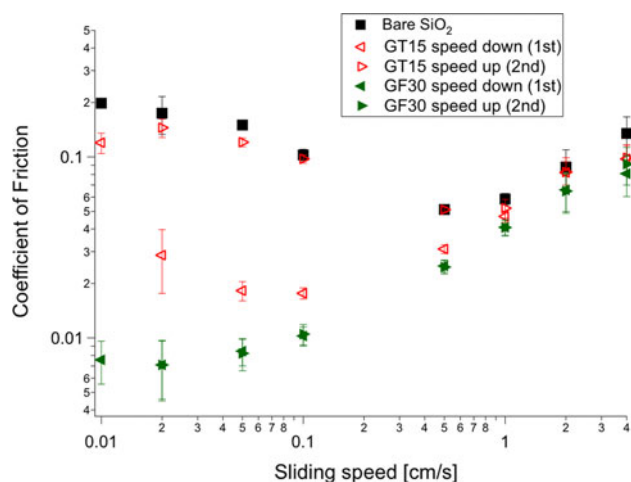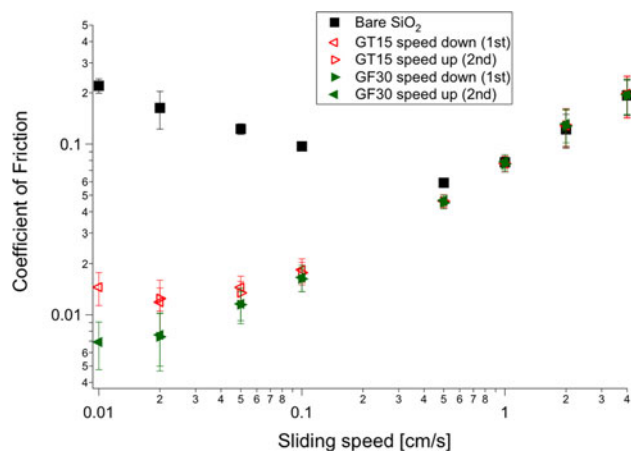The higher coating endurance observed at higher speeds or in higher viscosity oil suggests a time-dependent effect.

As discussed previously [10], the behaviour is reminiscent of the squeeze-film model of Hou et al. [19] for articular cartilage and synovial fluid systems and the apparent increase of viscosity of solvents in a polymeric network, observed by Feiler et al. [20]. The squeeze-film/enhanced viscosity model effectively describes lubrication with oil-compatible brushes: Prior to potential asperity–asperity contact, the pressure increases significantly and the oil is
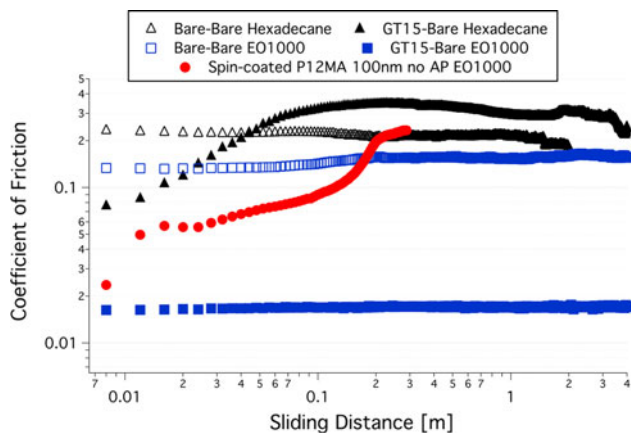
Fig. 8 Endurance test performed with polymer-coated silicon wafers slid against a bare borosilicate ball. A 100-nm-thick layer of P12MA, spin-coated onto the surface with no UV curing applied and without an adhesion promoter layer underneath is removed immediately, even in the viscous EO1000 oil

squeezed out of contact at a rate governed by the lubricant viscosity and its solvent–polymer interaction parameters. If the oil is sufficiently viscous, the asperities remain cushioned against each other under the specific load and viscosity conditions.

To complete the tribological characterisation of the grafting-to system, it was ensured that the lubricious properties of the grafted-to system arise from tethered coating, firmly attached to the surface, and not from loosely bound moieties. First, control experiments allowed us to verify that testing of the GT15 coatings can be interrupted and restarted after washing with toluene, the COF-distance curves continuing in an unaffected manner, thus demonstrating that any wear products present in the contact are not detrimental for the low-COF sliding. Second, tests with uncoated surfaces and a polymer-enriched oil (5 vol% of 470 kDa M_w P12MA in *EO500* oil) yielded COF values of 0.2 (typical for bare–bare at given conditions). This allowed us to exclude the possibility that the lubricating effect can be attributed to a free polymer present in the lubricating fluid due to wear processes, for example.

Finally, it is important to note that the low-coefficient-of-friction sliding on the grafted-to polymers only occurred when the complete grafting-to procedure was applied. In the absence of an adhesion-promoting layer, even a 100-nm-thick (spin-coated) P12MA coating tested in highly viscous (and therefore endurance-maximising) EO1000 lubricant was removed and no friction-reducing effect observed after a few cm of sliding (Fig. 8). Therefore, it is necessary that the spin-coated polymer is immobilised on the surface, for example, using a PAAm–PFPA adhesion-promoting layer.

4 Conclusions

In this study, we have compared the lubricating properties of similar polymers when attached via grafting-to and grafting-from approaches, and demonstrated an experimentally simple fabrication strategy for preparing lubricious, ultrathin, oil-compatible polymeric films. Despite the far less well-organised architectures of the surface-attached, spin-coated grafted-to P12MA films, in comparison to the grafted-from P12MA brush coatings prepared via SI-ATRP, they showed very effective lubricating properties, leading to COF values of ca 0.02 and non-detectable wear over 1,000 cycles, when slid against a bare silica sphere in oils of viscosity >500 cSt.

It was demonstrated that to separate asperities from potential hard–hard contact at a given speed, and therefore forestall the onset of coating wear, a lubricant of a certain minimal viscosity is needed, which is able to maintain a protective, soft, oil-swollen polymeric cushion. Further, the coating stability is related to the initial coating thickness, and thus even further extension of the operating speed, load and oil-viscosity ranges, for a given durability, would be foreseen upon increasing of the molecular weight of the spin-coated polymer.

References

1. Klein, J.: Shear of polymer brushes. Colloids Surf. A **86**, 63–76 (1994)
2. Binder, K., Kreer, T., Milchev, A.: Polymer brushes under flow and in other out-of-equilibrium conditions. Soft Matter **7**, 7159–7172 (2011)
3. Zhao, B., Brittain, W.J.: Polymer brushes: surface-immobilized macromolecules. Prog. Polym. Sci. **25**(5), 677–710 (2000)
4. Ma, H.W., Wells, M., Beebe, T.P., Chilkoti, A.: Surface-initiated atom transfer radical polymerization of oligo(ethylene glycol) methyl methacrylate from a mixed self-assembled monolayer on gold. Adv. Funct. Mater. **16**(5), 640–648 (2006)
5. Ulman, A.: Formation and structure of self-assembled monolayers. Chem. Rev. **96**, 1533–1554 (1996)
6. Fan, X.W., Lin, L.J., Dalsin, J.L., Messersmith, P.B.: Biomimetic anchor for surface-initiated polymerization from metal substrates. J. Am. Chem. Soc. **127**, 15843–15847 (2005)
7. Heeb, R., Lee, S., Venkataraman, N.V., Spencer, N.D.: Influence of salt on the aqueous lubrication properties of end-grafted, ethylene glycol-based self-assembled monolayers. ACS Appl. Mater. Interfaces **1**(5), 1105–1112 (2009)
8. Pasche, S., De Paul, S.M., Voros, J., Spencer, N.D., Textor, M.: Poly(L-lysine)-graft-poly(ethylene glycol) assembled monolayers on niobium oxide surfaces: a quantitative study of the influence of polymer interfacial architecture on resistance to protein adsorption by ToF-SIMS and in situ OWLS. Langmuir **19**(22), 9216–9225 (2003)
9. Saxer, S., Portmann, C., Tosatti, S., Gademann, K., Zürcher, S., Textor, M.: Surface assembly of catechol-functionalized poly(L-lysine)-graft-poly(ethylene glycol) copolymer on titanium exploiting combined electrostatically driven self-organization and

biomimetic strong adhesion. Macromolecules **43**(2), 1050–1060 (2010)

10. Bielecki, R.M., Crobu, M., Spencer, N.D.: Polymer-brush lubrication in oil: sliding beyond the stribeck curve. Tribol. Lett. 2012 (submitted). doi:10.1007/s11249-012-0059-9

11. Bielecki, R.M., Benetti, E.M., Kumar, D., Spencer, N.D.: Lubrication with oil-compatible polymer brushes. Tribol. Lett. **45**(3), 477–487 (2012)

12. Al-Bataineh, S.A., Luginbuehl, R., Textor, M., Yan, M.: Covalent immobilization of antibacterial furanones via photochemical activation of perfluorophenylazide. Langmuir **25**(13), 7432–7437 (2009)

13. Kubo, T., Wang, X., Tong, Q., Yan, M.: Polymer-based photo-coupling agent for the efficient immobilization of nanomaterials and small molecules. Langmuir **27**(15), 9372–9378 (2011)

14. Barbey, R., Lavanant, L., Paripovic, D., Schuewer, N., Sugnaux, C., Tugulu, S., Klok, H.: Polymer brushes via surface-initiated controlled radical polymerization: synthesis, characterization, properties, and applications. Chem. Rev. **109**, 5437–5527 (2009)

15. Ducker, W.A., Senden, T.J., Pashley, R.M.: Direct measurement of colloidal forces using an atomic force microscope. Nature **353**, 239–241 (1991)

16. Cannara, R.J., Eglin, M., Carpick, R.W.: Lateral force calibration in atomic force microscopy: a new lateral force calibration method and general guidelines for optimization. Rev. Sci. Instrum. **77**(5), 053701 (2006)

17. http://www.jawoollam.com. Accessed 7 Nov 2012

18. Zhang, Z., Morse, A.J., Armes, S.P., Lewis, A.L., Geoghegan, M., Leggett, G.J.: Effect of brush thickness and solvent composition on the friction force response of poly(2-(methacryloyloxy)ethylphosphorylcholine) brushes. Langmuir **27**, 2514–2521 (2011)

19. Hou, J.S., Mow, V.C., Lai, W.M., Holmes, M.H.: An analysis of the squeeze-film lubrication mechanism for articular-cartilage. J. Biomech. **25**(3), 247–259 (1992)

20. Feiler, A., Plunkett, M.A., Rutland, M.W.: Atomic force microscopy measurements of adsorbed polyelectrolyte layers. 1. Dynamics of forces and friction. Langmuir **19**(10), 4173–4179 (2003)